Proceedings of the Twenty-Ninth AAAI Conference on Artificial Intelligence

Pattern-Based Variant-Best-Neighbors Respiratory Motion Prediction Using Orthogonal Polynomials Approximation

Kin Ming Kam and **Shouyi Wang**
Department of Industrial, Manufacturing & Systems Engineering, University of Texas at Arlington, TX 76019

Stephen R Bowen
Department of Radiology and Integrated Brain Imaging Center, University of Washington, Seattle, WA 98195

Wanpracha Chaovalitwongse
Department of Industrial and Systems Engineering and the Integrated Brain Imaging Center, University of Washington, Seattle, WA 98195

Abstract

Motion-adaptive radiotherapy techniques are promising to deliver truly ablative radiation doses to tumors with minimal normal tissue exposure by accounting for real-time tumor movement. However, a major challenge of successful applications of these techniques is the real-time prediction of breathing-induced tumor motion to accommodate system delivery latencies. Predicting respiratory motion in real-time is challenging. The current respiratory motion prediction approaches are still not satisfactory in terms of accuracy and interpretability due to the complexity of breathing patterns and the high inter-individual variability across patients. In this paper, we propose a novel respiratory motion prediction framework which integrates four key components: a personalized monitoring window generator, an orthogonal polynomial approximation-based pattern library builder, a variant best neighbor pattern searcher, and a statistical prediction decision maker. The four functional components work together into a real-time prediction system and is capable of performing personalized tumor position prediction during radiotherapy. Based on a study of respiratory motion of 27 patients with lung cancer, the proposed prediction approach generated consistently better prediction performances than the current respiratory motion prediction approaches, particularly for long prediction horizons.

Introduction

In real-time image guided radiotherapy, respiratory motion can be a dominant factor for tumor movement (Ruan 2008). Without accounting for respiratory motion, critical misalignment between irradiated field and the target tumor volume in a treatment fraction may occur during radiotherapy, and impose significant radiation dose to normal body tissues. To account for respiratory motion in radiotherapy, real-time tumor-tracking systems have been developed to monitor tumor position in real-time and deliver therapeutic beam to the tumor accurately. Basically, a real-time tumor tracking system is designed to to perform three steps: (1) identify tumor position in real time; (2) reposition the beam; and (3) adapt the dosimetry to allow for changing lung volume and critical structure locations during the breathing cycle. However, it always suffers from some system time delay from real-time position tracking to therapeutic beam delivery. The system latency is the required response time of the whole system involving tasks such as image acquisition, motion estimation, hardware control and other factors (Keall et al. 2006; Ernst et al. 2013). As shown in Table 1, different real-time systems have different system latencies. The system latencies of four popular real-time radiotherapy systems range from 115 ms to 420 ms (Ernst 2011; Ernst et al. 2013). Such system latencies can lead to unnecessary irradiation of healthy tissues around the tumors. Accordingly, prediction of respiratory motion becomes a very critical issue in external beam radiotherapy to account for system specific latencies. However, predicting respiratory motion in real-time is challenging. The current respiratory motion prediction approaches are still not satisfactory in terms of accuracy and interpretability due to the complexity of breathing patterns and the high inter-individual variability across patients. In this study, we focused on the real-time respiratory motion prediction problem and developed a novel pattern-based variant-best-neighbors respiratory motion prediction system using orthogonal polynomial approximations and statistical analysis.

Table 1: A list of latancies of different systems.

	VERO	MLC	MAD	CyberKnife
Position acquisition	25	309	30	25
Position calculation	2	20	-	15
Gimbals/MLS/robot control cycle	20	52	45	75
Other	-	38	100	-
total	47	420	175	115

The main contributions of this work are: (1) formulate the respiratory motion prediction problem as a personalized pattern learning and recognition problem to fully account for the high inter-individual pattern variability across patients. (2) successful implementation of orthogonal polynomial approximations to achieve efficient real-time monitoring and recording respiratory patterns, (3) a variant-best-neighbors approach was developed to search the most significant predictive patterns using statistical analysis. Compared with the existing methods, the proposed prediction system achieved the most accurate and stable prediction performance according to the experiment of 27 patients.

Related Work

Many prediction methods for respiratory motion have been proposed in recent years. In this study, we have studied and reviewed the latest methods including Neural Networks (NN) (Krauss, Nill, and Oelfke 2011), Kernel Density Estimates (KDE) (Ruan 2010), Support Vector Regression Prediction (SVRpred) (Ernst and Schweikard 2009; Ernst et al. 2013), Recursive Least Squares (RLS) (Ernst et al. 2013), the MULIN algorithms (Ernst et al. 2013), normalized least mean squares, wavelet-based multiscale autoregression (wLMS) (Renaud, Starck, and Murtagh 2003; Ernst et al. 2013), Wavelet Neural Network (Chen, Yang, and Dong 2006), EKF Frequency Tracking. Most recently, Ichiji (Ichiji et al. 2012; 2013a; 2013b) proposed a Time Varying Seasonal Autoregressive Model with Adaptive Residual (resi-TVSAR) to adapt an AR model to time-varying situation. Ernst et al. (Ernst et al. 2013) did a comprehensive survey and comparison of the current respiratory motion prediction approaches, and found that the wLMS approach (Ernst, Schlaefer, and Schweikard 2007; Renaud, Starck, and Murtagh 2003) achieved the best prediction performance for short term prediction horizons, and the SVRpred approach (Ernst and Schweikard 2009) using online support vector regression (Renaud, Starck, and Murtagh 2003) obtained better prediction performance for longer prediction horizons. It is noted that support vector regression (SVR) is a currently popular approach in respiratory time series prediction (Choi et al. 2014; Ernst and Schweikard 2009; Ernst et al. 2013; Guo et al. 2013; Riaz et al. 2009; Smola and Schölkopf 2004; Bao, Xiong, and Hu 2014).

The Proposed Methods

Most of the current approaches only use recent respiratory cycles to train a prediction model to account for pattern variations over time. However, the whole respiratory motion record of a patient is not fully explored and much useful information in the past is not utilized. In this study, we propose a pattern-matching based framework to identify the similar patterns from the past respiratory record of a patient, make predictions based on statistical analysis of the 'future values' of the identified patterns from past record. Figure 1 shows the system diagram of the proposed prediction framework. Four functional components work together in real-time mode. A sliding window is applied to monitor real-time respiratory motion trajectory, a pattern library builder performs orthogonal polynomial approximation for the motion pattern within the sliding window, and stores the regression coefficients into the pattern library. The pattern library is growing over time as the sliding window monitors respiratory motion patterns of the patient. At each step of prediction, a pattern searcher searches a set of best-matching historical patterns in the pattern library to the motion pattern in the current sliding window. We consider the 'future values' of the best-matching historical patterns are useful to predict the future values beyond the current sliding window. Before prediction, an outlier analyzer is applied to make statistical analysis of the future values and eliminates the ones that are identified as outliers. Finally, a prediction decision maker integrates the 'future values' of the refined best patterns to make a prediction.

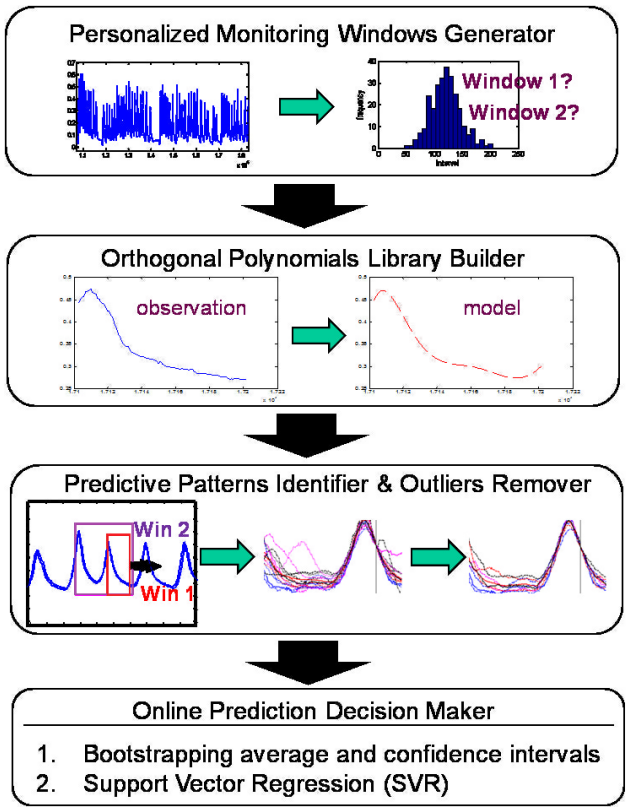

Figure 1: The general approach of the proposed pattern-based Variant-Best-Neighbors prediction by using raw data.

We propose a novel pattern-based variant best neighbors (VBN) method. For every sliding-window pattern, the number of best-matching neighbors in the pattern library is determined by a pattern-similarity criterion. As shown in Figure 1, before starting prediction, the first step is a training and validation process to determine the personalized pattern monitoring window length based on the statistics of the respiratory cycles of each individual patient. As the sliding window monitors respiratory motion trajectories over time, a pattern library is built by storing the monitored patterns in the sliding window. For each step of prediction, the best matching patterns are selected from the pattern library based on a pattern-similarity measure. This step provides the most matching patterns. The next step is to further refine the set of best neighbors(BNs) to enhance the prediction reliability using statistical analysis. After obtaining the BNs, we then use 'future values' of these patterns to make predictions. One can simply take the average of the 'future values' of the BNs or by applying support vector regression. The performance of both methods will be discussed in result section. Figure 2 illustrates the basic idea of the pattern-based prediction. Assume three best-matching patterns are identified to be similar to the current sliding window pattern at time t. For a prediction horizon of h steps, the predicted po-

sition at time $t+h$ is a function of the 'future values' of the three best matching neighbors as shown in the Figure.

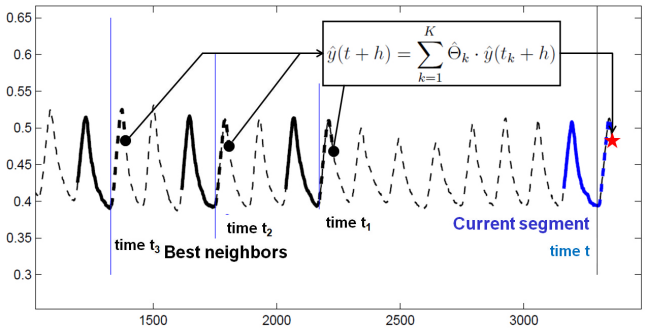

Figure 2: An example: by using pattern recognition approach, three best neighbors (solid black lines) of the current segment (solid blue line) are identified. By using the "future" values (the dotted lines) of the best neighbors, the prediction (red star) is made.

Orthogonal Polynomials Appximation

An orthogonal polynomial sequence is a family of polynomials such that any two different polynomials in the sequence are orthogonal to each other under some inner product (Chihara 2001). Due to convenient mathematical properties, we apply orthogonal polynomials to approximate respiratory motions patterns and do pattern matching correspondingly. The advantages of orthogonal polynomials approximations are: 1. fast determination of best order; 2. signal smoothing; 3. sparse data representation; 4. accurate approximation; 5. fast update and reconstruction; 6. ready for clustering and classification by using coefficients.

A time series consisting of real-valued samples y_t with $t = 0, ..., N$ with sampling rate, s, can be modeled by a parameterized function $f(x) : \mathbb{R} \to \mathbb{R}$. Here, we assume that $f(x)$ is linearly dependent on a parameter vector w with elements $w_k \in \mathbb{R}(k = 0, \ldots, K)$. Note that we do not claim that $f(x)$ is a linear function in x. More concretely, we assume that f is a linear combination of $K+1$ (linear or nonlinear) so-called basis functions f_k:

$$f(x) = \sum_{k=0}^{K} w_k \cdot f_k(x) \tag{1}$$

These basis functions may be polynomials, wavelets, sigmoid functions, or sinusoidal functions, for instance. We may write the values of the $K+1$ basis functions for the $N+1$ points in time $x_0, \ldots, x_N$ into a matrix

$$\mathbf{F} = \begin{pmatrix} f_0(x_0) & \cdots & f_K(x_0) \\ \vdots & \ddots & \vdots \\ f_0(x_N) & \cdots & f_K(x_N) \end{pmatrix} \tag{2}$$

If we combine the $N+1$ samples of the overall time series into a vector y with elements y_n, the linear least-squares problem we want to solve can be denoted by

$$\min_w \|\mathbf{Fw} - \mathbf{y}\| \tag{3}$$

with $\|\cdot\|$ being the euclidean norm. Its solution $\mathbf{w}_{LS}$ can be found by setting the derivative with respect to $\mathbf{w}$ to zero. First,

$$\begin{aligned} \|\mathbf{Fw} - \mathbf{y}\|^2 &= \langle \mathbf{Fw} - \mathbf{y} | \mathbf{Fw} - \mathbf{y} \rangle \\ &= \mathbf{w}^T\mathbf{F}^T\mathbf{Fw} - \mathbf{2y}^T\mathbf{Fw} + \mathbf{y}^T\mathbf{y} \end{aligned} \tag{4}$$

with $\langle \cdot | \cdot \rangle$ being the standard inner product in a real-valued vector space. Then,

$$\frac{\partial \|\mathbf{Fw} - \mathbf{y}\|^2}{\partial \mathbf{w}} = 2\mathbf{F}^T\mathbf{Fw} - \mathbf{2F}^T\mathbf{y} \tag{5}$$

leads to the least-squares solution

$$\mathbf{w}_{LS} = (\mathbf{F}^T\mathbf{F})^{-1}\mathbf{F}^T\mathbf{y} \tag{6}$$

In general, the solution of a linear least-squares problem is found by conducting a QR decomposition or a singular value decomposition (SVD) of $\mathbf{F}$. Now, assume that the selected $K+1$ basis functions are orthogonal with respect to an inner product yielding the value $\sum_{n=0}^{N} f_{k_1}(x_n)\dot{f}_{k_2}(x_n) = 0$ for any two basis functions f_{k_1} and f_{k_2} with $k_1 \neq k_2$. This is the case for special kinds of polynomials (see Section 3.2), for wavelet families, or the sinusoidal functions used for discrete Fourier transforms, for instance. Then,

$$\begin{aligned} \mathbf{F}^T\mathbf{F} &= \begin{pmatrix} f_0(x_0) & \cdots & f_0(x_N) \\ \vdots & \ddots & \vdots \\ f_K(x_0) & \cdots & f_K(x_N) \end{pmatrix} \begin{pmatrix} f_0(x_0) & \cdots & f_K(x_0) \\ \vdots & \ddots & \vdots \\ f_0(x_N) & \cdots & f_K(x_N) \end{pmatrix} \\ &= \begin{pmatrix} \|f_0\|^2 & \cdots & 0 \\ \vdots & \ddots & \vdots \\ 0 & \cdots & \|f_K\|^2 \end{pmatrix} \end{aligned} \tag{7}$$

That is: $\mathbf{F}^T\mathbf{F}$ is a diagonal matrix which can be inverted if the elements in the diagonal, which are the squared norms of the basis functions, are nonzero. This can be easily guaranteed by an appropriate choice of basis functions.

From 6, we then get

$$\begin{aligned} \mathbf{w}_{LS} &= (\mathbf{F}^T\mathbf{F})^{-1}\mathbf{F}^T\mathbf{y} \\ &= \begin{pmatrix} f_0(x_0)\frac{1}{\|f_0\|^2} & \cdots & f_0(x_N)\frac{1}{\|f_0\|^2} \\ \vdots & \ddots & \vdots \\ f_K(x_0)\frac{1}{\|f_K\|^2} & \cdots & f_K(x_N)\frac{1}{\|f_K\|^2} \end{pmatrix} \begin{pmatrix} y_0 \\ \vdots \\ y_N \end{pmatrix} \\ &= \begin{pmatrix} \sum_{n=0}^{N} \frac{y_n}{\|f_0\|^2} f_0(x_n) \\ \vdots \\ \sum_{n=0}^{N} \frac{y_n}{\|f_K\|^2} f_K(x_n) \end{pmatrix} \end{aligned} \tag{8}$$

That is the least-squares solution can be written as a linear combination of the training samples (cf. the dual representations of classifiers that are common in the field of support vector machines, for instance). Assume that, in a time window of length $L+1$, the values $y_0, y_1, \ldots, y_L$ measured at equidistant points in time $x_0, x_1, \ldots, x_L$ must be approximated by a polynomial f with degree $K \leq L (L \in \mathbb{N}_0, K \in \mathbb{N}_0)$ in the least-squares sense.

For sliding window method, the approximation window $[x_0, x_1, \ldots, x_M]$ is located at $[0, 1, \ldots, L]$. *Legendre* orthogonal polynomials are used in our study. Due to the orthogonality between OPs, the coefficients of OPs are independent to each other. So, if K^{th} order approximation has been done, we also obtain the approximations of all lower orders. This property empowers us to efficiently determine the best order of approximation. For each sliding window pattern, we first apply a 20th order approximation. To reduce the overfitting issue and smooth out noises, we reconstruct the respiratory motion pattern starting from order 1 until an order such that the approximation $R^2 > 0.95$. The coefficients of orders higher than this order are set to 0 when storing into the pattern library.

Personalized Pattern Monitoring Window Size

The interval is measured by the distance between consecutive peaks. The median of it is used as a baseline for window sizes of two-window design because of the skewness of the distribution of the interval.

To reasonably determine the final window size, we define a parameter which is the ratio of window size to the median of the intervals, R, to control the window size. The R is determined by validation. The window sizes are then multiplied by the selected ratio, $L = L_j \times R$ for $j = 1, 2$, i.e. Pattern libraries of all window size $B_{n \times L_j}$ are built up where n is the number of time segments in the library and L_j is the size of j^{th} window.

In validation process, one window ratio is picked each time. R-square is used for performance measurement because it provides a universal metric that describes how close the prediction is to the real data. The window ratio R that maximizes the R-square is selected for prediction.

$$\hat{R} = \arg\max_{R} \left[1 - \frac{\sum_{t=1}^{t=n} (\hat{y}(t, R) - \bar{y})^2}{\sum_{t=1}^{t=n} (y(t) - \bar{y})^2} \right] \quad (9)$$

Variant Best-Neighbors-Based Predictive Patterns

Phase I: Searching for Initial Best Neighbors By Using Right Aligned Patterns In phase I-1, the best-matched patterns are discovered by searching the pattern libraries of two window sizes, L_1 and L_2.

Using the current segment to look for patterns that their similarity measures, S defined as equation 11, satisfy a similarity threshold, θ. The baseline of candidates must be removed because we are only interested in their patterns. The regular VBN patterns have the problem of not considering signal shifting. Thus, it leads to inaccurate prediction due to the shifted errors as shown in left graphs of Figure 3. To achieve an accurate prediction, we propose to align the patterns at their rightmost point during VBN searching process. As shown in Figure 3, the right alignment puts higher weights on the right end and helps to obtain best neighbors that have a better match on the right end which is better for prediction.

$$\tilde{u}_n = u_n - u_n(end) \quad (10)$$

where u_n is the segment of n^{th} candidates in the pattern library and u_0 is the current segment. In this study, we introduce a usage of R-square as a similarity metric of two line segments.

$$S_n = 1 - \frac{SSE}{SStot} \quad (11)$$

while the sum of square of errors (SSE) is

$$\sum_{i=1}^{n} |e_i|^2 = \sum_{i=1}^{n} \left| \sum_{k=1}^{K} \Delta w_k (f_k(i) - f_k(n)) \right|^2 \quad (12)$$

By expansion, the SSE can be written in a close form:

$$SSE(\mathbf{w}) = c_{11} \Delta w_1^2 + c_{12} \Delta w_1 \Delta w_2 + \cdots + c_{kk} \Delta w_k^2 \quad (13)$$

where c_{jk} for $j, k \in 1, \ldots, K$ which are constants when the orthogonal polynomials, f_k, and n are fixed.

Figure 3 shows the close views of a typical example of best neighbors found by comparing raw patterns and right aligned patterns with the current segment. From Figure 3, we see that right aligned BNs give better prediction result. Even though the best neighbors found by raw patterns may show high similarity in overall but the right adjusted best neighbors show a better matching at the right side which is the closest point to the point that is going to be predicted.

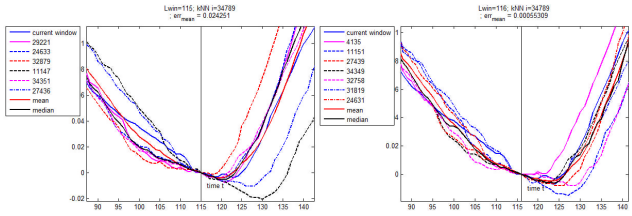

Figure 3: Online prediction of a patient's respiratory data by using unaligned BNs(Left) and right-aligned BNs(right).

Then, we sort the list S_n in ascending order to begin acquisition of BNs. We iteratively obtain the BNs from the top of the list until at least k BNs are obtained, and the next S_1 is smaller than the threshold, θ. One important thing has to be done is to remove the candidates that are adjacent to the selected BNs in order to prevent bias. Our removal strategy is shown as below:

$$B_k = \{u \in B_{k-1} | t_u < t_{\lambda_{k-1}} - m \cup t_u > t_{\lambda_{k-1}} + m\} \quad (14)$$

where B_k denotes the library at the time of after entering the k_{th} best neighbor; t_{λ_k} denotes the time at the end of k^{th} best neighbor λ; and m denotes a small distance that the candidates within this range are excluded. In the respiratory motion prediction study, we choose the distance as one-fifth of the median of the peak interval, i.e. $m = 0.2 \times median$. Then, a list of BNs, B_λ, is obtained at the end of Phase I.

Phase II: Best Neighbors Removal By Using Statistical Analysis Figure 4 shows the scatter plots of the errors of short segments before and after t_{λ_k} of the first six best neighbors of patient 23. This example demonstrates a phenomenon that the error at the right side is positively correlated to the error at the left side. Therefore, by further removing the candidates that have higher errors in the short

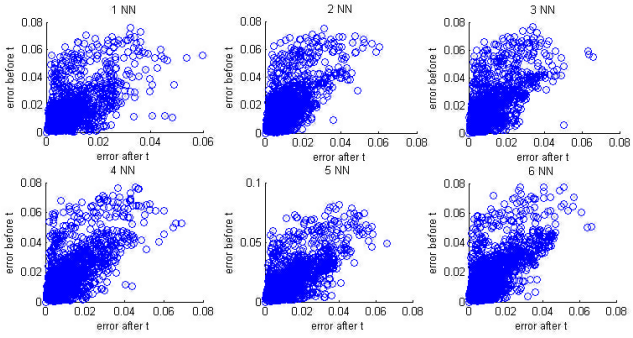

Figure 4: Scatter plots of the error before t_λ vs the error after t_λ of the first six nearest-neighbors. Correlation between the errors is observed.

term just before t_{λ_k}, the prediction performance can be enhanced.

The error of the mismatching of a short segment with length l just before and after time t are significantly correlated, where t_c is the current time point of the current segment and t_{λ_k} is the corresponding time points of k^{th} candidate. To further refine the set of the candidates, we suggest removing those candidates with bigger mismatching error of a few points just before time t. The square error of matching of a short segment of λ_k is shown as below:

$$d_{\lambda_k} = (D(t_c - l + 1 : t_c) - D(t_{\lambda_k} - l + 1 : t_{\lambda_k}))^2 \quad (15)$$

Next, since the distribution of error are skewed and the skewness varies among individuals, we remove the candidates with error larger than the median plus one and a half median absolute deviation(MAD) as follows:

$$\tilde{B} = \{\lambda \in B | d_\lambda <= d_{median} + 1.5 \times d_{MAD}\} \quad (16)$$

Although it is rare, sometimes the predicted value of a best-neighbor is an outlier among other candidates as shown in Figure 5. So, the last step of Phase II is to remove those candidates as follows:

$$\check{B} = \{\lambda \in B | D(t_\lambda + h) < \min(\max(D(t_\lambda + h)), P_{\lambda 75} + 1.5 \times (P_{\lambda 75} - P_{\lambda 25}))\} \quad (17)$$

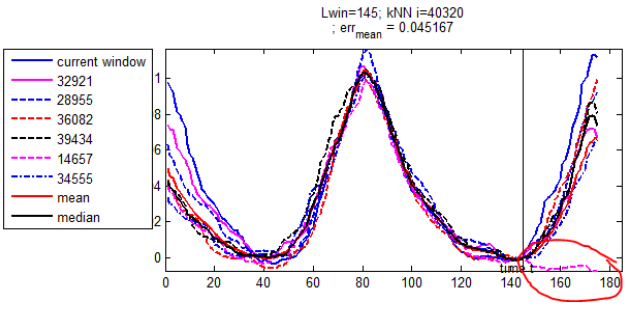

Figure 5: An example of an outlier amongst the best neighbors.

After finalizing the set of BNs, prediction is done by exploiting the information from them. The simplest and effective method is taking an average of their 'future values' as shown in equation 20.

Online Prediction Frameworks Using the Selected Predictive Patterns

Prediction Using Average of the Future Values of Reference Patterns For the best neighbors, the expected prediction values of h samples ahead is assumed to be similar.

$$E[y(t+h)] \simeq E[y(t_k+h)] \quad for \quad k = 1, \ldots, K \quad (18)$$

where K denotes the number of the similar patterns, $y(t_k + h)$ denotes the value at h samples ahead of k_{th} referenced pattern. Therefore, the prediction of h samples ahead made by using k best neighbors can be written as:

$$y(t+h) = \epsilon(t+h) + \sum_{k=1}^{K} \Theta_k \cdot y(t_k + h) \quad (19)$$

$\epsilon(t+h)$ denotes the error of predicting the value at time $t+h$ and Θ_k denotes the coefficient of the referenced value of k^{th} BN. $\epsilon(t+h)$ includes the random error and pattern mismatching error.

Taking the average of the referenced values, i.e. the samples that are h samples ahead of all BNs, for prediction, the proposed model equation can be written as:

$$\hat{y}(t+h) = \sum_{k=1}^{K} \hat{\Theta}_k \cdot \hat{y}(t_k + h) \quad (20)$$

We set $\Theta_k = \frac{1}{K}$ to use the mean of the future values of the referenced patterns for prediction. We name the proposed Right-Aligned Pattern VBN-Based Mean Prediction as OPPRED and RPKM for the ones using orthogonal polynomials approximation and using raw data respectively.

Experimental Results

In our experiments, we compare the prediction performance of the proposed methods, i.e. RPKM and OPPRED, and the latest state-of-the-art methods, i.e. wLMS, SVRpred and TVSAR. In addition, Seasonal ARIMA is also added to the comparison as most people are familiar to this method.

Data Acquisition and Experimental Settings

Time series of abdominal displacement of 27 lung and liver cancer patients were collected with the Real-time Position Management^{TM}(RPM)(Varian Inc., Santa Clara, CA) infrared camera and reflective marker block system during their PET/CT examination. The time series serves as a respiratory motion surrogate (Wang, Gwizdka, and Chaovalitwongse 2014). The sampling rate of respiratory traces was 30 Hz. The duration of data collection was from 15 to 45 minutes. The respiratory motion traces of 27 patients demonstrated very high individuality.

For TVSAR and wLMS, they do not need training. Prediction directly started at the testing set. For the experiment of RPKM and OPPRED, the personalized window size has to be determined before prediction. Also, in the experiment, the similarity threshold θ is set to be 0.95. For SVRpred, we consider $-2^{12}, -2^{11}, \ldots, 2^{12}$ for kernel parameter, γ, and $0, 0.01, 0.02, \ldots, 0.1$ for insensitive zone, ϵ, and $\max(|\bar{y} + 3\sigma_y|, |\bar{y} - 3\sigma_y)$ for regularization parameter, C.

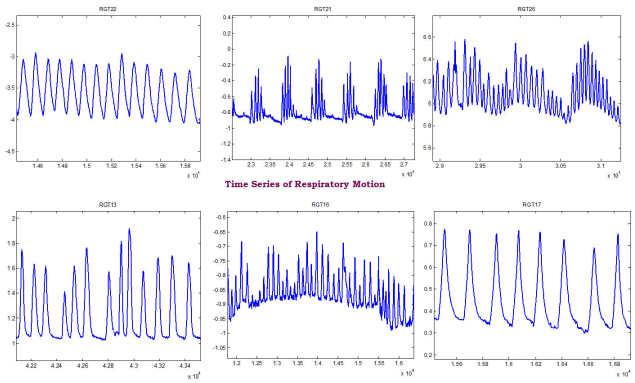

Figure 6: Examples of respiratory motion patterns from six patients that show the tremendous inter-individual pattern variability.

Prediction Performance of RPKM, OPPRED and the latest state-of-the-art methods

Table 2 shows the prediction performances of RPKM, OPPRED, res_TVSAR, wLMS, SVRpred and SARIMA. And, Figure 7 to Figure 9 are the box plots of the prediction performance of the proposed methods and the current state-of-the-art methods for 27 patients. From boxplots, both in terms of the mean level and the inter-variation of prediction performance of RPKM and OPPRED are significantly better than all other methods. Among the state-of-the-art methods, wLMS performs very well in short term prediction and res_TVSAR outperforms wLMS for long term prediction. Except SVRpred, all other methods perform better than SARIMA. From Figure 7 to Figure 9, one can observe that the RPKM and OPPRED approaches significantly outperform the current methods in all prediction horizons.

Table 2: Prediction performance comparison for the proposed approaches and the state-of-the-art of respiratory motion prediction methods with respect to four prediction horizons: 1, 5, 10 and 15 steps. Each step is $\frac{1}{30}$ seconds.

Prediction horizon (steps)		1	5	10	15
RPKM	mean	0.998	0.976	0.918	0.831
	std	0.001	0.018	0.052	0.095
OPPRED	mean	0.998	0.975	0.914	0.824
	std	0.001	0.019	0.056	0.100
res_TVSAR	mean	0.964	0.834	0.684	0.462
	std	0.088	0.378	0.393	0.436
wLMS	mean	0.996	0.880	0.648	0.386
	std	0.005	0.322	0.487	0.527
SVRpred	mean	0.908	0.738	0.639	0.347
	std	0.044	0.075	0.099	0.164
SARIMA	mean	0.979	0.846	0.608	0.231
	std	0.019	0.127	0.281	0.469

Discussion and Conclusion

In this study, we developed a pattern-based variant-best-neighbors respiratory motion prediction system using orthogonal polynomial approximations and statistical analysis.

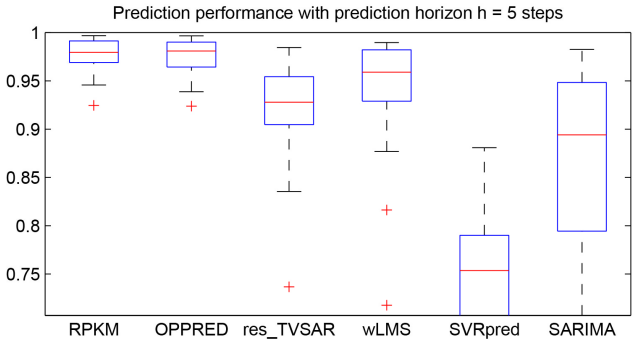

Figure 7: Prediction performance of RPKM, OPPRED, res_TVSAR, wLMS, SVRpred and SARIMA (h=5 steps).

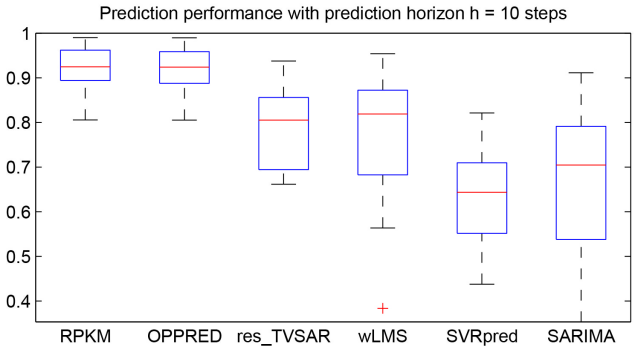

Figure 8: Prediction performance of RPKM, OPPRED, res_TVSAR, wLMS, SVRpred and SARIMA (h=10 steps).

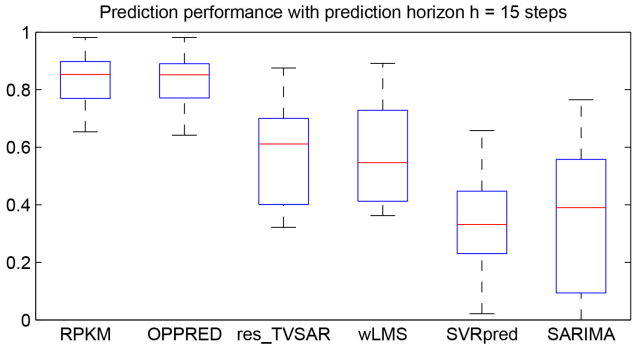

Figure 9: Prediction performance of RPKM, OPPRED, res_TVSAR, wLMS, SVRpred and SARIMA (h=15 steps).

In real-time radiotherapy, system latencies need to be compensated for accurate irradiation during treatment. Accurate respiratory motion prediction can minimize the damage of normal body tissues and important human organs. The proposed approach can effectively utilize the relevant information from the whole respiratory record of a patient. The orthogonal polynomial approximations have been successfully implemented to achieve efficient real-time monitoring and recording respiratory patterns. And the variant-best-neighbors approach showed its effectiveness to search the most significant predictive patterns using statistical analysis. The experimental results confirmed that the proposed prediction methods outperform all other methods significantly

which gives a great impact on respiratory motion time series prediction for radiotherapy.

References

Bao, Y.; Xiong, T.; and Hu, Z. 2014. Multi-step-ahead time series prediction using multiple-output support vector regression. *Neurocomputing* 129:482–493.

Chen, Y.; Yang, B.; and Dong, J. 2006. Time-series prediction using a local linear wavelet neural network. *Neurocomputing* 69(4):449–465.

Chihara, T. 2001. 45 years of orthogonal polynomials: a view from the wings. *Journal of computational and applied mathematics* 133(1):13–21.

Choi, S.; Chang, Y.; Kim, N.; Park, S. H.; Song, S. Y.; and Kang, H. S. 2014. Performance enhancement of respiratory tumor motion prediction using adaptive support vector regression: Comparison with adaptive neural network method. *International Journal of Imaging Systems and Technology* 24(1):8–15.

Ernst, F., and Schweikard, A. 2009. Forecasting respiratory motion with accurate online support vector regression (svrpred). *International journal of computer assisted radiology and surgery* 4(5):439–447.

Ernst, F.; Dürichen, R.; Schlaefer, A.; and Schweikard, A. 2013. Evaluating and comparing algorithms for respiratory motion prediction. *Physics in medicine and biology* 58(11):3911.

Ernst, F.; Schlaefer, A.; and Schweikard, A. 2007. Prediction of respiratory motion with wavelet-based multiscale autoregression. *Medical Image Computing and Computer-Assisted InterventionMICCAI 2007* 668–675.

Ernst, F. 2011. *Compensating for quasi-periodic Motion in robotic radiosurgery*. Springer.

Guo, S.; Lucas, R. M.; Ponsonby, A.-L.; et al. 2013. A novel approach for prediction of vitamin d status using support vector regression. *PloS one* 8(11):e79970.

Ichiji, K.; Homma, N.; Sakai, M.; Takai, Y.; Narita, Y.; Abe, M.; and Yoshizawa, M. 2012. Respiratory motion prediction for tumor following radiotherapy by using time-variant seasonal autoregressive techniques. *Engineering in Medicine and Biology Society (EMBC), 2012 Annual International Conference of the IEEE* 8:6028–6031.

Ichiji, K.; Homma, N.; Sakai, M.; Abe, M.; Sugita, N.; and Yoshizawa, M. 2013a. A respiratory motion prediction based on time-variant seasonal autoregressive model for real-time image-guided radiotherapy.

Ichiji, K.; Homma, N.; Sakai, M.; Narita, Y.; Takai, Y.; Zhang, X.; Abe, M.; Sugita, N.; and Yoshizawa, M. 2013b. A time-varying seasonal autoregressive model-based prediction of respiratory motion for tumor following radiotherapy. *Computational and mathematical methods in medicine* 2013.

Keall, P. J.; Mageras, G. S.; Balter, J. M.; Emery, R. S.; Forster, K. M.; Jiang, S. B.; Kapatoes, J. M.; Low, D. A.; Murphy, M. J.; Murray, B. R.; et al. 2006. The management of respiratory motion in radiation oncology report of aapm task group 76a). *Medical physics* 33(10):3874–3900.

Krauss, A.; Nill, S.; and Oelfke, U. 2011. The comparative performance of four respiratory motion predictors for real-time tumour tracking. *Physics in medicine and biology* 56(16):5303.

Renaud, O.; Starck, J.-L.; and Murtagh, F. 2003. Prediction based on a multiscale decomposition. *International Journal of Wavelets, Multiresolution and Information Processing* 1(02):217–232.

Riaz, N.; Shanker, P.; Wiersma, R.; Gudmundsson, O.; Mao, W.; Widrow, B.; and Xing, L. 2009. Predicting respiratory tumor motion with multi-dimensional adaptive filters and support vector regression. *Physics in medicine and biology* 54(19):5735.

Ruan, D. 2008. *Image guided respiratory motion analysis: time series and image registration*. ProQuest.

Ruan, D. 2010. Kernel density estimation-based real-time prediction for respiratory motion. *Physics in medicine and biology* 55(5):1311.

Smola, A. J., and Schölkopf, B. 2004. A tutorial on support vector regression. *Statistics and computing* 14(3):199–222.

Wang, S.; Gwizdka, J.; and Chaovalitwongse, W. A. 2014. Using physiological signals to assess mental motion for tumor following radiotherapy. *IEEE TRANSACTIONS ON HUMAN-MACHINE SYSTEMS*.